2023 IEEE/ASME International Conference on Advanced Intelligent Mechatronics (AIM)
June 28-30, 2023. Seattle, Washington, USA

Application of Support Vector Machine for Near Real-Time Health Structural Diagnosis for Drones

Wei-Hsiang Lai
Department of Aeronautics and Astronautics
National Cheng Kung University
Tainan 701, Taiwan
whlai@mail.ncku.edu.tw

Yih-Rong Liang
Department of Aeronautics and Astronautics
National Cheng Kung University
Tainan 701, Taiwan
p46091254@ncku.edu.tw

Carlos Rene Cristales Cardona
Department of Aeronautics and Astronautics
National Cheng Kung University
Tainan 701, Taiwan
p46107102@gs.ncku.edu.tw

De-Li Cheng
Department of Aeronautics and Astronautics
National Cheng Kung University
Tainan 701, Taiwan
z11005016@ncku.edu.tw

***Abstract*— A real-time health structural diagnosis system for drones is becoming a key factor in developing safe drone operations and technologies. This study is dedicated to building one. Drone health status can be real-time diagnosed as "non-fault" or "potential fault" status. This study adds extra IMU sensors to collect the vibration signal of different drone structural faults and extracts the time domain and frequency domain features of the signal through feature engineering methods. Then, a Support Vector Machine (SVM) model is trained with those features. Feature selection and hyper-parameter tuning methods have been applied during model training to prevent model overfitting. This study also integrates a Window Sliding Technique and MAVLink to improve the real-time health diagnosis system.**

Keywords—UAV, Structural Health Diagnosis, Real-Time Diagnosis, SVM, Machine Learning, Window Sliding Technique.

I. INTRODUCTION

Technology advancements and the race by major drone companies to launch less-expensive and well-functioning Unmanned Aerial Vehicles (UAV) have led to a boom in multi-axis drones in recent years. However, under this rapid development, most users cannot identify the health status of drones, so safety concerns have gradually increased. According to the research statistics of Gorucu [1], the number of registered drones in the United States has exceeded 1.7 million by 2020. From 2015 to the end of 2019, about 4,250 people were injured in drone-related flight accidents.

Different damage types or factors affect the flight safety of multi-rotor UAVs; Gopi Kandaswamy [2] divided drone faults into three types. The first type is electronic glitches, such as electromagnetic field interference, remote control or GPS signal interference, barometer abnormality, and other temporary fault conditions. The second type is electronic faults, such as the inertial measurement unit, magnetic compass, additional sensors in the flight control system, or the failure of the flight control system itself and the battery. And the third type is a structural fault, such as the drone body, motor, and propeller failure. Yong Keong Yap and others [3,4,6] monitored the fuselage structure health of a UAV and divided it into three fault states, loose blades, loose screws of the motor base, and damaged blades. In addition, he incorporated an IMU next to the motor, collected the acceleration under three different fault states and different rotational speeds and performed spectrum analysis with Fast Fourier transform (FFT), then found out the vibration characteristics in different states, and carried out the health diagnosis of the power system of the UAV.

The above literature shows that the existing research on damage identification of UAVs takes the power system of the UAV as the primary identification focus. It can be found that the damage characteristics of the power system of the UAV in the fault state can be collected by accelerometer or audio. Then Fast Fourier Transform, statistics, and other methods can be used to extract and analyze the characteristics of the signal. In terms of multi-rotors, Adam Bondyra [8] used the Fast Fourier transform, WPD (Wavelet Packet Decomposition), and Band Power, three signal processing methods to obtain the characteristics of the damaged state of the propeller of a four-axis small UAV. Overall, the vibration signal is an important indicator when analyzing the rotating mechanism or the body structure of the drone, so this study uses the vibration signal as the basis for establishing the health diagnosis model.

The study of UAV health diagnosis can be divided into two research directions, real-time health diagnosis and long-term health diagnosis [9]. The main characteristic of real-time health diagnosis is fast calculation speed, but the diagnostic accuracy is lower. In real-time diagnosis, traditional machine learning or control theory can be applied to establish a diagnosis model. Additionally, long-term health diagnosis characteristics are high accuracy and powerful classification performance. Still, the calculation time of the diagnosis is long, and the hardware demand is higher. However, these characteristics allow the use of highly recognizable features and advanced machine learning algorithms.

This paper aims to present a real-time health diagnosis system for UAVs. This system uses real-time vibration signals to extract its features and conduct a preliminary health diagnosis through an SVM machine learning algorithm so that users can instantly identify the presence of a fault. This paper is organized as follows. In Section II, time domain and frequency domain features are introduced. Section III outlines the equipment employed in this study, including the experimental process. In Section IV, the process of feature selection, model hyper-parameter tuning, and model training are explained, and the preliminary performance indicators of the model are demonstrated. The results are described and discussed in Section V, and conclusions are presented in Section VI.

II. Materials and Methods

A. Feature Engineering

As per D.L. Cheng and Muhammad Masood Tahir's literature [10], Feature Engineering is employed to extract time-domain and frequency-domain features from the sensor's original data through mathematical and statistical methods to create a new data set. Then Feature Selection is applied to select only those features with high correlation to improve the performance of the model. This study adopts six feature extraction methods in the time domain and one feature extraction method in the frequency domain.

1) Time Domain Feature Engineering

Root Mean Square, Standard Deviation, Variance, Skewness, Kurtosis, Sample Entropy.

2) Frequency Domain Feature Engineering

Fast Fourier Transform.

3) Feature Selection

As the number of features increases, we have more information for our model. However, too many features may demand high-end hardware and increase the probability of model overfitting. Therefore, we need to maintain the features that have a high correlation with our target and exclude the ones that don't.

At present, the main feature selection methods can be divided into Filter Methods, Wrapper Methods, and Embedded Methods. The feature selection method used in this study is based on the Wrapper Method. The purpose of the Wrapper Method is to create a variety of possible feature sets, perform model training with each set, and then use a set of verification data to validate the model performance and continue iterating until the best-performing feature set is found.

III. Experimental Process

A. Experimental Setup

This chapter will describe the experimental equipment used in this research. The system architecture diagram is shown in Fig. 3.1, which comprises the UAV and the embedded computer systems. Each system will be introduced in the subsequent sections.

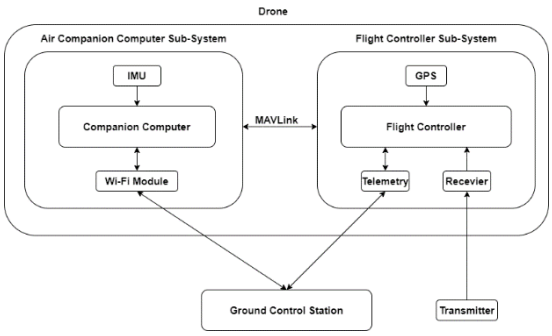

Fig. 3.1. System architecture diagram.

1) UAV System

The UAV employed in this experiment is shown in Fig. 3.2. The details of its components are listed in Table I.

Fig. 3.2. UAV employed in the experiment.

2) Companion Computer System

The companion computer system integrates a Raspberry Pi computer and an external inertial measurement unit (IMU). In this study, Raspberry Pi 4 Model B is used to collect acceleration data from the external IMU and the airborne embedded device that calculates the health status of the UAV.

The IMU used in this research is the BerryIMU v3, which is a 6-axis IMU based on LSM6DSL. The output frequency of the accelerometer was set at 3.33 kHz and transmitted through the SPI interface. The measurement range was set at ±8 g with a Nyquist Frequency of 1.66 kHz [18], which represents the highest frequency observed in the vibration signal.

B. Definition of Health Status

1) Potential fault

This study divides the UAV faults into three types: motor base screw loosening, propeller damage, and propeller mount screw loosening, shown in Fig 3.4.

Screw loosening is a fault that has a great impact on flight safety. The possible reasons for loosening include wear of the thread or not properly locking the parts during assembly, etc., which may cause the relative position of the motor and the arm to change. This can lead to a crash due to an unstable flight. In this experiment, the tightness of the screws in the motor base and the machine arm was changed to simulate the screw loosening fault of the motor base. In this state, the motor is not able to balance the torque at the bottom, and that causes additional vibration, Fig 3.4a.

The propeller is one of the most easily damaged parts of the drone, and the surface is often scratched or damaged due to impact during operation, as shown in Fig 3.4b. These phenomena cause abnormal vibrations when the drone is flying. If it is significant, it will affect flight safety; in addition, when users install the propeller, it is often prone to accidents because the screw is not fully locked, as shown in Fig 3.4c.

Since the objective of this research is to diagnose the health status of UAVs, the potential fault state will be defined as, among the above three types of faults, the UAV has at least one, and the severity of the fault can be witnessed by human eyes or hands.

2) Non-fault

After defining the potential fault state, this study defines the following two conditions as the non-fault state. First, the drone does not have the above three faults, and second, the drone can fly stable.

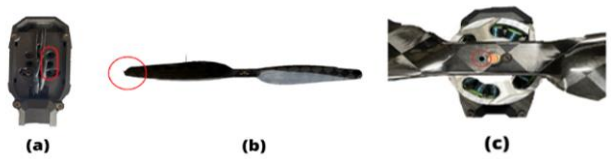

Fig. 3.4. Types of drone faults: (a) motor base screw loosening; (b) propeller damage; (c) propeller mount screw loosening.

C. Flight Experiment

1) Flight Environment and Experimental Conditions

The three following restrictions were set during the experiment to ensure the consistency of external conditions when collecting flight data. First, the outdoor wind speed was below 5.4 m/s (Beaufort wind scale 4), which has a higher tolerance for the environment than the 2 m/s set by S.T. Tsai [5], and is more in line with reality; second, during the flight, we ensured that the voltage of each Li-Po battery cell was not lower than 3.7V, to ensure the flight safety of the drone and to prevent the data being affected by the battery power; thirdly, all the flight experiments in this research were carried out in GPS mode (Loiter Mode). This mode automatically attempts to maintain the current position, heading, and altitude of the drone, which is very user-friendly for general flight tasks.

2) Flight Experiment Process

The flight experiment is conducted as follows: first, set one of the UAV health statuses described in Table I which also lists the flight time ratio for each health status; second, manually unlock the UAV, switch it to Waypoint mode, and execute the planned flight path. The UAV automatically takes off to a position 5 meters above the ground and continues to fly to the next waypoint. After the set time is completed, it will automatically switch to Land mode and perform landing; following the above steps, the user only needs to change the health status of the drone in step one to complete the data collection.

TABLE I. UAV HEALTH STATUS FLIGHT TIME RATIO

Health Status	Definition	Flight Time Ratio
Non-fault	There are no faults, and it can fly stably	50%
Motor base screw loosening	The two screws of the motor base are loose	10%
Broken propeller	The propeller is slightly damaged	10%
Propeller mount screw loosening	A single screw of the propeller is loose	10%
Hybrid fault	Three states of random mixing faults	20%

D. Feature Extraction

1) Data Preprocessing

The general flight record file (Log) stores plenty of data during the flight, including altitude, altitude change, throttle values, etc., this log file is stored in the SD card of the flight control board, but unfortunately, even though we can access measurements from the flight controller's IMU via programming, the sampling rate is still around 1400 Hz due to high computational cost, which is still not adequate for classifying. For that reason, an external IMU connected to a Raspberry Pi was placed at the center of the drone. This will provide a more symmetrical measurement of the overall vibration levels, taking into account the vibrations from all four rotors and the drone's frame. The IMU acceleration measurements will then be the raw data that can be used to extract the relevant features to train the model.

This research focuses on extracting features from the acceleration data, but in the collection process, in addition to collecting the vibration signal of the UAV fuselage, the acceleration data of the UAV altitude changes during flight is also captured. Therefore, the signal captured before the propeller of the UAV starts rotating must be removed. This study uses the Python high-pass filter function to remove the vibration signals below 5Hz, and only retains the vibration signals of the drone body.

2) Feature Processing

Following data pre-processing, the seven feature engineering methods introduced in Section II of this article were applied to the processed vibration signal in the XYZ directions. There are three features per feature extraction method. A total of 21 features were obtained. After feature extraction is completed, it is necessary to use the standard score (Z-score) method to standardize the 21 types of features respectively, and then complete all feature processing steps, which will be followed in the next section.

IV. MODEL BUILDING AND ANALYSIS

This study uses the SVM machine learning algorithm to build the classification model. After the vibration signal runs through the feature extraction methods described in previous sections, data can be divided into 80% of the data set for training the model and 20% to test the performance of the model.

When building a model, in addition to the final performance of the model, whether the model is overfitting or underfitting is also an essential factor to consider. Therefore, k-Fold Cross Validation was used during model training to reduce the possibility of overfitting and, at the same time, have a more realistic model performance.

In addition, if the model-building steps are simplified, it can significantly affect the model performance. There are two blocks: first, the data used to build the model, and second, setting the parameters of the model; this paper uses a Sequential Feature Selector algorithm to select the data that will eventually be used to train the model.

A. Cross-validation

In this study, k-Fold Cross Validation (CV) was used for evaluating the model performance, the training data set is divided into k sets ($k=5$ for our model), leaving one of the k sets as the validation data set, the remaining k - 1 sets are used as training data. After the model training is completed, the validation data set is used to test the model's performance and obtain a performance value. Finally, the above steps are repeated in k splits, and all the performance values obtained in each split are averaged; the averaged model performance will be able to show the actual performance of the model more comprehensively and will not be misled by extreme values due to the factor of data partitioning.

B. Feature Selection

In Machine Learning, selecting the most important and highly relevant features and excluding the less relevant ones can reduce the probability of overfitting, shorten the training time, and even improve the performance of the model. Therefore, Python's sklearn SequentialFeatureSelector function was used for feature selection.

As mentioned in previous sections, 21 features were extracted from the original vibration signal. After using the feature selection method mentioned above, 12 features were selected as the final feature set for this study, shown in Table II.

TABLE II. FEATURE SELECTION RESULTS

No.	Direction	Feature	No.	Direction	Feature
1	X	Root mean square	7	X	Kurtosis
2	X	Standard deviation	8	Y	Kurtosis
3	Y	Standard deviation	9	Z	Kurtosis
4	Z	Standard deviation	10	X	Fast Fourier Transform
5	X	Variation	11	Y	Fast Fourier Transform
6	Z	Variation	12	Z	Fast Fourier Transform

C. SVM Parameter Selection

There are 32 possible permutations and combinations of model parameters, as shown in Table III. In this part, the GridSearchCV function from the sklearn Python library was used to select the SVM model parameters.

TABLE III. SVM MODEL PARAMETER LIST

Variable	Possible testing values			
Kernel Function	Polynomial	RBF		
Penalty Coefficient C	1	10	100	1000
Gamma	Scale	0.1	0.01	0.001

After parameter selection, the Radial Basis Function (RBF) was selected, with a penalty coefficient C of 100 and Gamma set to Scale, which means that the model judges the value by itself according to the training data set.

D. SVM Model Results

This section analyzes the final performance of the model. After using 80% of the data set to train the model, 20% of the data set was used to let the model predict, then a confusion matrix was employed for analysis, as shown in Table IV. Table V lists the performance indicators of the SVM model, and this study uses the recall rate as the primary performance indicator.

TABLE IV. HEALTH DIAGNOSIS MODEL CONFUSION MATRIX

Predict / Actual	Non-fault	Potential fault	Recall rate
Non-fault	734	288	72%
Potential-fault	159	1754	92%

TABLE V. HEALTH DIAGNOSIS MODEL PERFORMANCE INDICATORS

Accuracy	85%
Precision	86%
Recall	92%
F1 score	89%

It can be seen from Table IV that the model has a high recall rate of 92% for the potential fault state but only 72% for the non-fault state. This might occur because the potential fault state features are not only hardly observable faults but also slightly similar to the non-fault state ones, resulting in more non-fault states that the model judges as potential fault states. However, this result is still in line with the set goal, which is to have a higher recall rate for the potential fault state.

V. EXPERIMENTAL RESULTS AND ANALYSIS

To achieve the purpose of this research, which is to detect UAV potential faults in real-time, the performance of the health diagnosis model in predicting new data and the sliding window method application to actual flight missions will be examined.

A. Predicting with New Data

In the experiment of predicting new data, we re-collected a relatively similar amount of flight data with non-fault and potential fault status, and its confusion matrix is shown in Table VI. The recall rate was still 86%, while the non-fault recall rate was reduced to 65%. The overall trend is still the same as the results in Table IV. It had a good recall rate performance with a potential fault status but a slightly lower recall rate with non-fault status; if we compare the prediction results of the SVM health diagnosis model with original and new data, as shown in Fig. 5.1, it can be found that the recall rate of the model for new data is reduced by about 7%. A possible reason is that the flight environment was different when collecting new data, which led to a slight decrease in the recall rate.

TABLE VI. CONFUSION MATRIX OF HEALTH DIAGNOSIS MODEL PREDICTING WITH NEW DATA

Predict / Actual	Non-fault	Potential fault	Recall rate
Non-fault	1388	752	65%
Potential fault	210	1262	86%

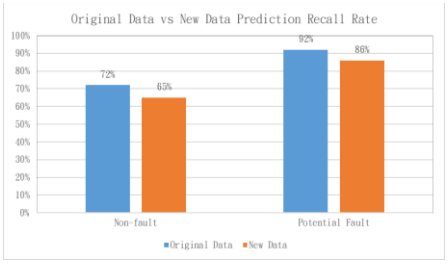

Fig. 5.1. Original and new data health diagnosis prediction recall rate comparison.

B. Individual Fault assessment

To understand the prediction performance of the health diagnosis model for individual types of faults, the prediction results of four different health states will be listed separately. Table VII defines the four different health states. For comparison, see Fig. 5.2; according to the results in part A of Section V, the recall rate of new data is slightly lower than that

of the original data, but it can be found in Fig. 5.2 that when the health status of the drone is motor base and propeller mount screws loosening, the recall rate increases significantly. The possible reason for this phenomenon is that on the day of collecting new data, the ambient wind speed was significantly higher, which caused the drone to increase the motor speed and vibration to maintain the posture of the drone, leading to a higher recall rate for some damage states.

TABLE VII. INDIVIDUAL HEALTH STATUSES DESCRIPTION

No.	Health Status	Definition
1	Non-fault	There are no faults, and it can fly stably
2	Motor base screw loosening	The two screws of the motor base are loose
3	Broken propeller	The propeller is slightly damaged
4	Propeller mount screw loosening	A single screw of the propeller is loose

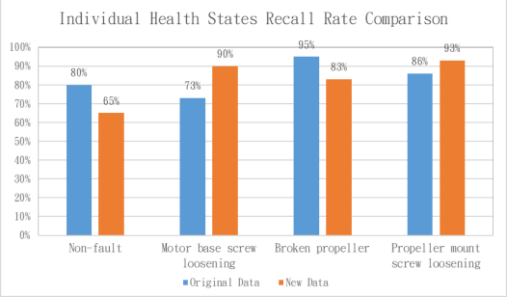

Fig. 5.2. Health diagnosis model recall rate comparison for the prediction of individual health statuses.

C. Sliding Window Application

The system for monitoring UAV fault state must continuously evaluate for potential faults. However, if the system has a relatively low recall rate for non-fault conditions, users may be troubled by excessive warnings while flying in complex conditions. To address this issue, the non-fault recall rate must be improved. One approach is to use a sliding window, which allows for a more comprehensive analysis of data. In this method, all outputs within the window must indicate a potential fault to identify a likely fault state. Otherwise, the state will be considered non-fault. Table VIII illustrates that increasing the sliding window range results in a requirement for more consecutive equal outputs, leading to a decrease in potential fault state recall rate but a significant improvement in non-fault state recall rate.

TABLE VIII. APPLICATION OF THE SLIDING WINDOW RANGE TO THE CHANGE OF THE RECALL RATE

No.	Health Status	Sliding window range						
		1	2	3	4	5	6	7
1	Non-fault	65%	78%	84%	88%	91%	94%	95%
2	Potential fault	86%	75%	66%	60%	59%	49%	45%

The application of a sliding window method aligns more closely with the two key requirements of the UAV instant diagnosis system. It must accurately detect potential faults while also avoiding the constant output of false positives when the UAV is in a non-fault state. From Table VIII, we can see that a sliding window size of 6 achieves a non-fault state recall rate close to 95% and a potential fault state recall rate close to 50%. Therefore, this study sets the sliding window range to 6. Although the potential fault recall rate of 49% may seem low, Table VI shows that when the UAV has a potential fault, the recall rate is 86%. This indicates that the model can accurately judge a fault condition continuously, which could serve as an early indicator for the user.

The method proposed by [6] shares some similarities with the method presented in this study, but also differs in several key aspects. While both methods focus on structural health diagnosis, Cheng's method relies on post-flight analysis, which may not be convenient for early fault detection. In contrast, the method proposed in this study can perform real-time diagnosis, enabling early detection and prevention of potential accidents. While the accuracy of the other author's method is higher than the approach presented in this study, the real-time diagnosis capability of our method offers a significant advantage over post-flight analysis, as it allows for quick and effective detection of structural faults during UAV flight.

D. UAV Real-Time Health Diagnosis System

After completing all the building steps, this study incorporates the health diagnosis model into the UAV to achieve a real-time structural health diagnosis system. After the system starts to execute and connects with the flight controller through the MAVLink communication protocol, it will first detect whether the drone is unlocked, which means that the propeller of the drone is rotating, then the accelerometer will collect 3200 samples per second. These data are normalized and passed through feature extraction, then imported into the model, and the model defines the current health status of the drone. If the drone status is healthy, the drone is in a non-fault state, and the steps of data collection and diagnosis are repeated continuously. If the drone status is unhealthy, it means that the UAV might have a potential fault, and the variable F in the system that continuously determines the UAV's potential fault state will be increased by 1. If the number of consecutive potential fault outputs reaches 6 times, follow-up actions will be executed at the end.

E. Flight Tests

In the actual flight test, because the health status of the UAV cannot be changed during flight, the experimental procedure was as follows: first, the health status of the UAV is preset as no fault or potential fault before take-off; The drone takes off automatically using the waypoint mode, and automatically executes the waypoint task for about 1 minute. Third, immediately after the drone takes off, the real-time health diagnosis system starts diagnosing the health status of the drone; if the diagnosis is a potential fault state, then it will display a message on the embedded system terminal to notify the user and will automatically switch to landing mode to perform automatic landing, otherwise, it will automatically land after completing all waypoint tasks.

1) Non-Fault State Test

In this test, the health status of the UAV before take-off was a non-fault state. The yellow box in Fig. 5.3 shows that the embedded system and the flight controller are successfully connected. The picture also shows how the system begins to diagnose and the number of times the system has continuously diagnosed the potential fault in the UAV. Still, because the system did not diagnose potential faults more than six times to

the waypoint, the UAV automatically followed the waypoint until it normally landed and then shut off.

2) Potential Fault State Test

In this test, the health status of the UAV before take-off was a potential fault state. The red box in Fig. 5.3 portrays how the system continuously diagnosed that the UAV had a potential fault six consecutive times. Therefore, the UAV real-time health diagnosis system actively changed the flight mode of the UAV to Land mode, performed automatic landing, and then shut off.

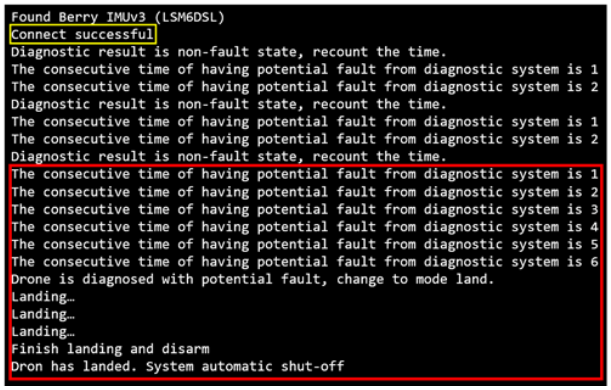

Fig. 5.3. UAV real-time health diagnosis system running screen.

F. Limitations

One of the main limitations of this method is the potential cost associated with using a single-board computer, such as the Raspberry Pi, for data collection and analysis. While these devices have become increasingly affordable in recent years, they may still represent a significant expense for some users. Additionally, the use of external sensors, such as the IMU used in this study, is restricted to compatibility with the Raspberry Pi computer. This may limit the availability of alternative or superior sensors that could provide more accurate or comprehensive data for UAV health monitoring. These limitations highlight the need for further research to develop more cost-effective and versatile methods for UAV health monitoring that can accommodate a wider range of sensors and data collection methods.

VI. Conclusions

This study successfully established a near real-time structural health diagnosis system for drones based on vibration analysis. Experiments demonstrated that the system could reach a potential fault prediction recall rate of 86% when predicting with new data. It has been revealed that the sliding window technique can accommodate the wind disturbance conditions captured by the sensors, increasing the prediction recall rate of the model. The connection between the embedded system and the flight controller through MAVLink improves the health diagnosis by not only alerting the user about fault occurrence but also performing an emergency landing.

Based on the conducted research, we address the accuracy of the model to the sampling rate of the sensors. Therefore, our future goal is to employ higher sampling rate sensors to achieve greater structural diagnosis accuracy. The scope selection and diversity of training data could have also been factors that influenced wind resilience and accuracy. We will also delve into this subject in the future.

References

[1] S. Gorucu, Y. Ampatzidis, “Drone Injuries and Safety Recommendations”, UF/IFAS Department of Agricultural and Biological Engineering, vol 2021, No 3, 2021.

[2] G. Kandaswamy, P. Balamuralidhar, “Health Monitoring and Failure Detection of Electronic and Structural Components in Small Unmanned Aerial Vehicles” *World Academy of Science, Engineering and Technology International Journal of Mechanical and Mechatronics Engineering*, Vol.11, No.5, pp.1080-1089. 2017.

[3] Y.K. Yap, “Structural Health Monitoring for Unmanned Aerial Systems” *Technical Report No. UCB/EECS-2014-70.* Electrical Engineering and Computer Sciences University of California at Berkeley, 2014.

[4] S.T. Tsai, “Application of Wavelet Scattering and Machine Learning on Flight Data Analysis for Quadcopter Diagnosis Classification System”, National Cheng Kung University Master's Thesis, 2020.

[5] C. Ge, K. Dunno, M.A. Singh, L. Yuan and L. X. Lu. "Development of a Drone’s Vibration, Shock, and Atmospheric Profiles" *Applied Sciences*, 11(11), p 5176, 2021.

[6] D.L. Cheng , “Application of Self-Organizing Map on Flight Data Analysis for Quadcopter Health Diagnosis System”, National Cheng Kung University Master's Thesis, 2019.

[7] M. Bronz, E. Baskaya, D. Delahaye, S. Puechmorel, “Real-time Fault Detection on Small Fixed-Wing UAVs using Machine Learning”, *DASC 2020 AIAA/IEEE 39th Digital Avionics Systems Conferenc*e, October, pp.1～10, 2020.

[8] A. Bondaradyra, P. Gasior, S. Gardecki and A. Kasiński, "Fault diagnosis and condition monitoring of UAV rotor using signal processing," *2017 Signal Processing: Algorithms, Architectures, Arrangements, and Applications (SPA)*, pp.233～238, 2017.

[9] Y. Lai, B. Yang, X. Jiang, F. Jia, N. Li, A. K. Nandi, “Applications of machine learning to machine fault diagnosis: A review and roadmap”, *Mechanical Systems and Signal Processing*, 138, 106587, 2020.

[10] M.M. Tahir, S. Badshah, A. Hussain, M. A. Khattak,” Extracting accurate time domain features from vibration signals for reliable classification of bearing faults”, *International Journal of Advanced and Applied Sciences*, 5(1), pp.156～163, 2018.

[11] J.S. Richman, J. R. Moorman, “Physiological time-series analysis using approximate entropy and sample entropy.” *American journal of physiology. Heart and circulatory physiology*, 278(6), 2000.

[12] J.W. Cooley, J.W. Tukey , “An algorithm for the machine calculation of complex Fourier series.” *Mathematics of Computation*, 19, pp.297～301, 1965.

[13] C. Cortes, V. Vapnik, “Support-vector networks. ” *Machine Learning*, 20, pp.273～297, 1995.

[14] S.R. Gunn, “Support vector machines for classification and regression,” *ISIS technical report*, 14(1), pp.5～16, 1998.

[15] H.R. Baghaee, D. Mlakić, S. Nikolovski and T. Dragicević, "Support Vector Machine-Based Islanding and Grid Fault Detection in Active Distribution Networks", *IEEE Journal of Emerging and Selected Topics in Power Electronics*, vol. 8, no. 3, September, pp.2385-2403, 2020.

[16] A. Raza, A. Dhakal, S. Honkanen, R. Baets, “Glucose sensing using photonics waveguide based evanescent Raman spectroscopy”, University of Ghent, Ughent, Belgium, 2015.

[17] H. Cramér, Probability and Statistics: The Harald Cramér Volume, Almqvist & Wiksell, 1959.